

Cover Page



Universiteit Leiden



The handle <http://hdl.handle.net/1887/25142> holds various files of this Leiden University dissertation.

**Author:** Temviriyankul, Piya

**Title:** Translesion synthesis : cellular and organismal functions

**Issue Date:** 2014-04-10

# CHAPTER

# 5

## GENOME INSTABILITY FOLLOWING MITOTIC TRANSMISSION OF UNREPLICATED DNA LESIONS

Piya Temviriyankul, Sandrine van Hees-Stuivenberg, Anastasia Tsaalbi-Shtylik,  
Jacob G. Jansen and Niels de Wind

*Manuscript in preparation*

## ABSTRACT

Replication stress can lead to the generation of double stranded DNA breaks (DSBs) that are correlated with loss of genetic information, structural chromosomal aberrations and tumorigenesis. Here, we have investigated the mechanistic basis of these structural alterations using mammalian cells defective in nucleotide excision repair and post-replicative bypass of DNA lesions as models. We show that, upon treatment with ultraviolet (UV) light, cells accumulate patches of ssDNA containing (6-4)pyrimidine pyrimidone photoproducts ((6-4)PPs) in genomic DNA. Rather than rapidly collapsing into DSBs, these ssDNA gaps are transmitted through mitosis into the subsequent cell cycle. During the ensuing S phase, the ssDNA gaps are converted into DSBs, leading to genomic instability.

## INTRODUCTION

Genomic DNA is continuously damaged by cellular by-products such as oxygen radicals and by exogenous agents such as ultraviolet light (UV), X-rays and genotoxic substances. In replicating cells, DNA lesions that have escaped removal by appropriate DNA repair pathways may form impregnable obstructions for replicative DNA polymerases  $\delta$  and  $\epsilon$ , leading to arrested replication forks. Prolonged fork stalling can lead to dissociation of the replisome and fork collapse, resulting in the formation of DNA double-stranded breaks (DSBs) (Chapman *et al.*, 2012). DSBs are believed to arise when stalled replication forks are converted into aberrant DNA structures that are cleaved by structure-specific endonucleases (Hanada *et al.*, 2007; Osman *et al.*, 2007). Persistent DSBs activate DNA damage signaling pathways that induce cell cycle delay, senescence or apoptosis. In addition, the generation of DSBs is strongly correlated with loss of genetic information, as evidenced by the appearance of micronuclei (MN), and with other structural chromosomal aberrations. Such genomic instability is associated with tumorigenesis (Bonassi *et al.*, 2007; Murgia *et al.*, 2008).

To prevent prolonged stalling of replication forks at sites of unrepaired DNA damage, cells are equipped with DNA damage tolerance (DDT) pathways, i.e. DNA damage avoidance (DA) and translesion synthesis (TLS). DDT thereby allows cells to complete replication of damaged DNA templates, precluding genomic instability (Sale *et al.*, 2012; Waters *et al.*, 2009). In bacteria, stalled forks are predominantly and accurately rescued from collapsing by DA, which involves template switching to the undamaged sister chromatid (Berdichevsky *et al.*, 2002; Izhar *et al.*, 2008). In higher eukaryotes TLS appears to be a more dominant DNA damage tolerance pathway (Izhar *et al.*, 2013; Szuts *et al.*, 2008). TLS utilizes specialized DNA polymerases, so-called TLS polymerases, that are capable of inserting nucleotides opposite, and extending beyond, DNA lesions, thereby enabling DNA damage bypass. TLS, though, is an intrinsically error-prone process, due to the extended active sites, the low selectivity of nucleotide incorporation and the lack of proofreading activity of TLS polymerases (Waters *et al.*, 2009). Thus, TLS contributes to cell survival at the cost of genome instability. TLS most likely bypasses mildly helix-distorting DNA lesions directly at the replication fork. Strongly helix-distorting DNA lesions, such as UV-induced (6-4) pyrimidine pyrimidone photoproducts ((6-4)PPs), can be bypassed independently from chromosomal replication, via post-replicative filling of single-stranded DNA (ssDNA) gaps that are caused by repriming of the replisome downstream of the fork-blocking DNA lesion or by convergence of a replication fork from an adjacent origin of replication (Daigaku *et al.*, 2010; Jansen *et al.*, 2009).

The TLS polymerase Rev1 plays a central role in TLS in eukaryotic cells. Rev1 is shown to be essential for the bypass of UV-induced (6-4)PP and of BPDE-induced DNA lesions *in vivo* (Temviriyankul *et al.*, 2012a; Temviriyankul *et al.*, 2012b; Zhao *et al.*, 2006). In addition, cells deficient for Rev1 are hypomutable by different DNA damaging agents, indicating that Rev1 is important for mutagenic TLS across helix-distorting

DNA lesions (Jansen *et al.*, 2009; Washington *et al.*, 2004; Yang *et al.*, 2009; Zhang *et al.*, 2002). It is believed that Rev1 functions mostly as a scaffold protein for other TLS polymerases to perform TLS across fork-blocking DNA lesions (Sale *et al.*, 2012; Waters *et al.*, 2009). Presumably, Rev1 is involved in post-replicative gap-filling in yeast and mammalian cells, since (i) the expression of Rev1 is the highest in the G2 phase in yeast (Waters *et al.*, 2006), (ii) Rev1-dependent TLS can act independent of chromosomal replication (Diamant *et al.*, 2012), and (iii) following UV exposure, Rev1-deficient mouse embryonic fibroblasts (MEFs) accumulate ssDNA gaps containing (6-4)PPs during S phase progression (Jansen *et al.*, 2009).

Recently, we reported that the generation of ssDNA gaps containing (6-4)PPs in proliferating Rev1-deficient MEFs is accompanied with increased DNA damage signaling, a delay in cell cycle progression, enhanced formation of MN and hypersensitivity to UVC light (Temviriyankul *et al.*, 2012b). Thus, Rev1-deficient cells appear good models to study the induction of DNA damage responses and of genome instability, by replication stress. Here, we employed an integrative approach to monitor the fate of ssDNA gaps containing (6-4)PPs and their impact on genomic integrity at well-defined stages during the first and second cell cycles after UVC exposure. To further sensitize these cells to replication stress, MEF lines used here were additionally defective in nucleotide excision repair, by a targeted disruption of the *Xpc* gene (Cheo *et al.*, 1997).

We provide evidence that ssDNA gaps opposite (6-4)PPs can persist in mitotic chromatin. After transfer through mitosis, these lesion-containing gaps are converted into DSBs in the ensuing S phase, which is accompanied with massive DNA damage signaling. These data reveal a novel pathway for the collapse of stalled replication forks. In addition, these results may have profound implications for genotoxicity testing of chemical and physical agents using the MN assay.

## RESULTS

### Delayed Formation of Micronuclei in *Rev1*<sup>-/-</sup>*Xpc*<sup>-/-</sup> MEFs After Exposure to a Low Dose of UVC

To study the fate of stalled forks at UVC-induced (6-4)PPs, we assayed the induction of micronuclei (MN) in *Xpc*<sup>-/-</sup> and *Rev1*<sup>-/-</sup>*Xpc*<sup>-/-</sup> MEFs (Jansen *et al.*, 2009). MN are abnormal extracellular bodies resulting from DSBs-induced chromosome breaks or from mis-segregation of whole chromosomes into daughter cells during cell division. MN thereby are specific and sensitive indicators of chromosome instability, relevant for tumorigenesis (Bonassi *et al.*, 2007; Murgia *et al.*, 2008). MEFs were mock treated or exposed to a low or high dose of UVC (0.4 and 5 J/m<sup>2</sup>) and immediately cultured in the presence of the cytokinesis-blocking agent cytochalasin-B (cyt-B). Of note, the 0.4 J/m<sup>2</sup> dose induces similar toxicity in *Rev1*<sup>-/-</sup>*Xpc*<sup>-/-</sup> MEFs to the 5 J/m<sup>2</sup> dose in *Xpc*<sup>-/-</sup> MEFs (Fig. 1A). After 24h, binucleated (BN) cells, that have undergone mitosis, were

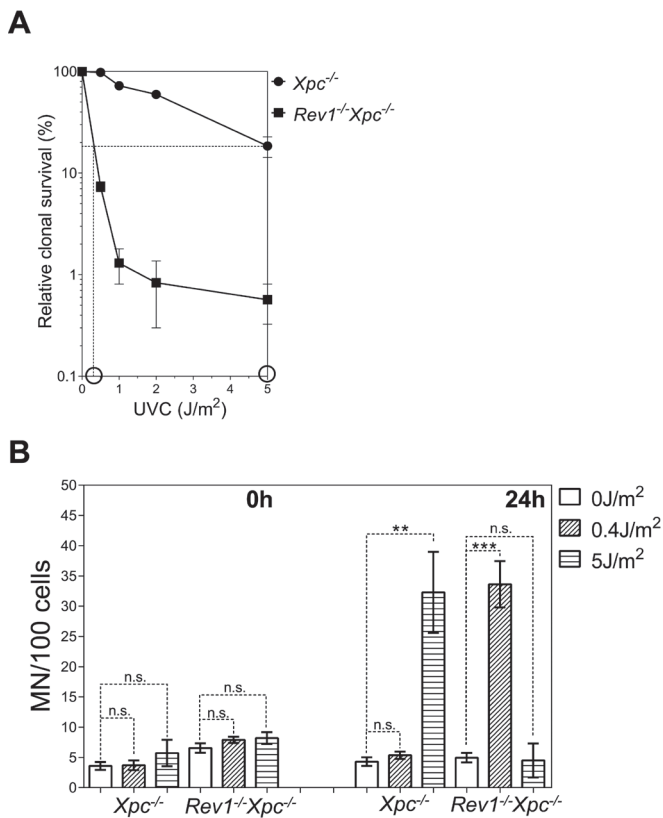


**Figure 1 | UVC hypersensitivity and the late formation of MN in *Rev1*<sup>-/-</sup>*Xpc*<sup>-/-</sup> MEFs exposed to low doses of UVC.** (A) Relative clonogenic survival of cells treated with different doses of UVC. The cloning efficiency of mock-treated cells was set as 100% ( $n=3$ ). Circles indicate an equitoxic UVC dose for *Xpc*<sup>-/-</sup> and *Rev1*<sup>-/-</sup>*Xpc*<sup>-/-</sup> MEFs. Cells were treated with different doses of UVC or mock-treated, and then cyt-B was added, at 0h (left panel) or 24h (right panel) after treatment. Twenty-four hours later, cells were fixed and the induction of MN in binucleated cells was scored. Bars represent the number of MN per 100 cells after exposure to UVC or mock treatment ( $n=3$ ). Error bar, SEM. Statistical significance was analyzed by Student's *t*-test against mock treated. \*\*,  $p<0.01$ ; \*\*\*,  $p<0.001$ , n.s., non significant.

analysed for the induction of MN. Surprisingly, no induction of MN was observed for either cell line following exposure to either dose of UVC (Fig. 1B). We then added cyt-B at only 24h after UVC exposure, followed by an additional incubation of 24h. Under these conditions *Rev1*<sup>-/-</sup>*Xpc*<sup>-/-</sup> MEFs, exposed at 0.4J/m<sup>2</sup>, displayed 7-fold more MN than its mock-treated control. *Xpc*<sup>-/-</sup> MEFs displayed no MN induction at this UVC dose (Fig. 1B). Conversely, at 5J/m<sup>2</sup> UVC, MN induction in *Xpc*<sup>-/-</sup> MEFs was approximately 6 times higher than its mock-treated control, whereas *Rev1*<sup>-/-</sup>*Xpc*<sup>-/-</sup> MEFs exhibited background levels of MN (Fig. 1B). Together, these results suggest that equitoxic UVC doses induce genome instability, irrespective of the Rev1 status, but in all genetic backgrounds only late after exposure.

### Progression of *Rev1*<sup>-/-</sup>*Xpc*<sup>-/-</sup> MEFs Into The Second Cell Cycle Upon a Low Dose of UVC

We then investigated cell cycle progression in these MEF lines exposed to 0, 0.4 and 2J/m<sup>2</sup> UVC. After treatment, replicating cells were pulse-labeled with BrdU, to enable to track cell cycle progression of individual cells. Then, cells were fixed at indicated times. At 8h after mock treatment, all cells progressed to the subsequent G1 phase at a similar rate, suggesting that loss of Rev1 does not affect cell cycle progression of undamaged cells (Fig. 2 and supplementary Fig. S1). Progression of *Xpc*<sup>-/-</sup> MEFs to the subsequent G1 phase was not affected by exposure to a low dose of 0.4J/m<sup>2</sup> UVC, whereas exposure to 2J/m<sup>2</sup> slightly and transiently delayed progression (Fig. 2 and supplementary Fig. S1). *Rev1*<sup>-/-</sup>*Xpc*<sup>-/-</sup> MEFs displayed a very transient reduction in the progression towards G1, at 8h after exposure of S phase cells to 0.4J/m<sup>2</sup> UVC. Very slow recovery and cell cycle progression was seen when *Rev1*<sup>-/-</sup>*Xpc*<sup>-/-</sup> MEFs were exposed to 2J/m<sup>2</sup> UVC, indicating that the DNA damage load irreversibly affects cell cycle progression in *Rev1*<sup>-/-</sup>*Xpc*<sup>-/-</sup> MEFs at a higher UVC dose. These results suggest that the delayed induction of MN is correlated with cell cycle progression of damaged cells, upon exposure to equitoxic UVC doses of *Xpc*<sup>-/-</sup> and *Rev1*<sup>-/-</sup>*Xpc*<sup>-/-</sup> MEFs.

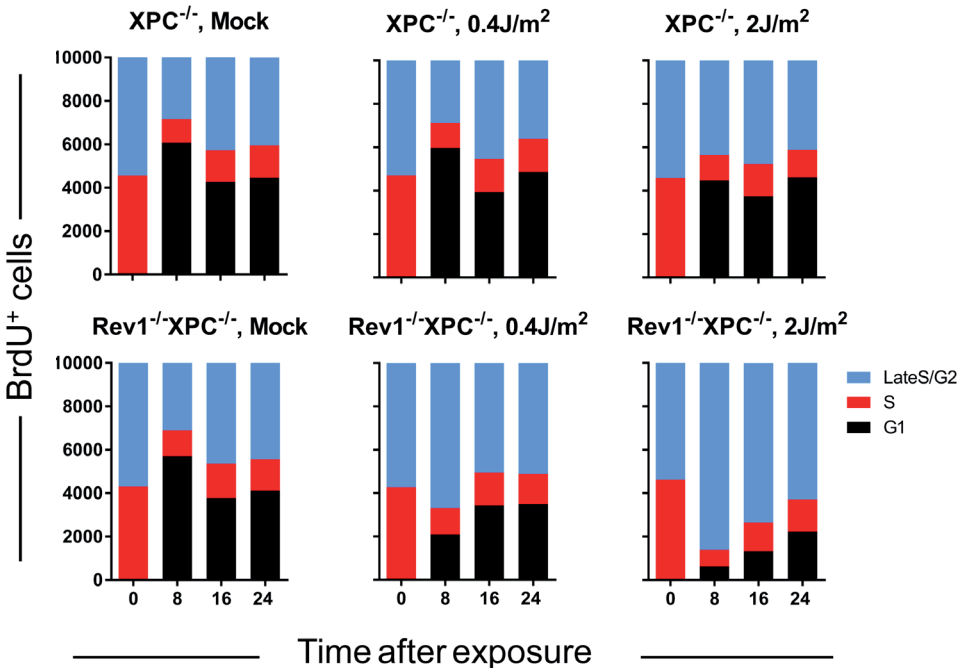


**Figure 2 | *Rev1*<sup>-/-</sup>*Xpc*<sup>-/-</sup> MEFs can progress to the second cell cycle upon low doses of UVC irradiation.** Cells were pulse-labeled with BrdU, immediately after UVC exposure (up to 2J/m<sup>2</sup>) or mock-treated. Then, cells were analyzed by flow cytometer. BrdU-positive cells in G1, S and late S/G2 phases were quantified, at different times up to 24h after treatment.

### UVC Induces Genome Instability Only in The 2<sup>nd</sup> S phase Upon Exposure

We considered the possibility that UVC-induced genome instability becomes apparent only during the 2<sup>nd</sup> cell cycle after exposure. This possibility was addressed using a double-labeling MN assay protocol. This protocol relies on the finding that cyt-B inhibits cytokinesis but does not preclude cell cycle progression in daughter nuclei of binucleated cells (Estensen, 1971; Fournier *et al.*, 1975). MEFs were treated with 0 or 0.4J/m<sup>2</sup> UVC, pulse-labeled with BrdU to mark cells that were replicating during UVC treatment and cultured for 24h in normal medium, allowing the cells to enter the next cell cycle (Fig. 2). Then, the cells were pulse-labeled with the replication marker EdU, to enable to identify cells in the 2<sup>nd</sup> S phase after exposure, and cultured in the presence of cyt-B for a further period of 24h prior to fixation and analysis of MN induction (Fig. 3A(i) for a scheme). We infer that binucleated cells, double-positive for BrdU and EdU (BrdU<sup>+</sup>/Edu<sup>+</sup>), have finished the 2<sup>nd</sup> cell cycle upon UVC treatment during S phase.

No induction of MN was seen in BrdU<sup>+</sup>/Edu<sup>+</sup> *Xpc*<sup>-/-</sup> control MEFs after either mock or UVC treatment, consistent with the results from the classical MN assay (see above). However, at the same UV dose, binucleated BrdU<sup>+</sup>/Edu<sup>+</sup> *Rev1*<sup>-/-</sup>*Xpc*<sup>-/-</sup> MEFs displayed a significant induction of MN after UVC treatment, *i.e.* about 8 times higher than the mock-treated control and *Xpc*<sup>-/-</sup> MEFs (Fig. 3B). To exclude the possibility that these MN are derived from DSBs generated in the first, rather than the second, cell cycle, we analyzed MN in MEFs that were exposed to 0 or 0.4J/m<sup>2</sup> UVC, then pulse-labeled with BrdU, and immediately cultured for only 24h in the presence of cyt-B to enable to visualize MNs in first-cycle cells. Just before fixation, the cells were pulse-labeled with EdU. Binucleated BrdU<sup>+</sup>/EdU<sup>-</sup> *Rev1*<sup>-/-</sup>*Xpc*<sup>-/-</sup> cells have not entered yet the second S phase after UVC exposure (Fig. 3A(ii) for a scheme). In this cell population, the frequency of MN was not increased, excluding the possibility that the MNs arise during the first cycle (Fig. 3C). Together, these results suggest that *Rev1*<sup>-/-</sup>*Xpc*<sup>-/-</sup> cells acquire genome instability only during the second cell cycle following exposure during S phase to UVC light.

### Unreplicated (6-4)PPs Persist Beyond Mitosis

We hypothesized that ssDNA interruptions at (6-4)PP can persist throughout the cell cycle. To investigate this, we first measured DNA strand interruptions in mitotic cells using the alkaline comet assay (McKelvey-Martin *et al.*, 1993). Thus, *Xpc*<sup>-/-</sup> and *Rev1*<sup>-/-</sup>*Xpc*<sup>-/-</sup> MEFs were exposed to 0, 0.4 and 2J/m<sup>2</sup> UVC followed by pulse labeling with BrdU to mark cells that are replicating during UVC treatment. Cells were then cultured in the presence of nocodazole for 16h to accumulate cells at the first mitosis after exposure. This nocodazole treatment is important to exclude comets of S phase cells from the analysis. Then, cell suspensions were subjected to gel electrophoresis under alkaline conditions and tail moments of BrdU-containing nuclei, representing all DNA strand interruptions, were quantified. For mock-treated cells, both genotypes showed similar tail moments, suggesting the presence of only low amounts of

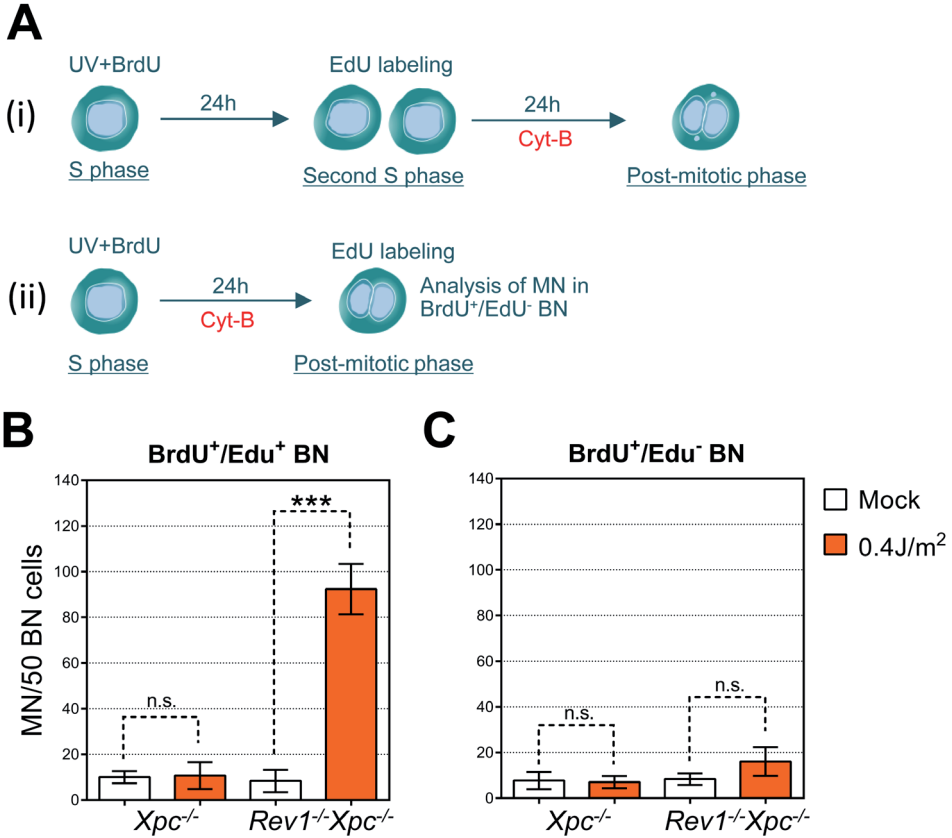


**Figure 3 | Induction of DSBs in the 2<sup>nd</sup> S phase of *Rev1*<sup>-/-</sup>*Xpc*<sup>-/-</sup> MEFs exposed to UVC.** (A) Experimental schemes to identify BN cells derived from UV-exposed cells that have completed (i) two cell cycles (BrdU<sup>+</sup>/EdU<sup>+</sup> BN cells) or (ii) one cell cycle (BrdU<sup>+</sup>/EdU<sup>-</sup> BN cells). (B) Quantification of MN in BrdU<sup>+</sup>/EdU<sup>+</sup> BN cells. (C) Quantification of MN in BrdU<sup>+</sup>/EdU<sup>-</sup> BN cells. Bars represent the number of MN per 50 cells after exposure to UVC or mock treatment ( $n=3$ ). Error bar, SEM. Statistical significance was determined by Student's *t*-test. \*\*\*,  $p < 0.001$ , n.s., non significant.

DNA strand discontinuities in non-exposed cells (Figs. 4A and B). In *Xpc*<sup>-/-</sup> MEFs treated with doses of up to 2J/m<sup>2</sup> of UVC no increase in tail moments was observed. *Rev1*<sup>-/-</sup>*Xpc*<sup>-/-</sup> MEFs, however, displayed a UV dose-dependent increase in tail moments in the alkaline comet assay. Neutral comet assays, that detect only DSBs, did not show any increase of tail moments in UVC-exposed *Rev1*<sup>-/-</sup>*Xpc*<sup>-/-</sup> MEFs compared with mock-treated cells (Figs. 4A and B), confirming that measurable levels of DSBs are not generated during the first cell cycle after UVC exposure. Based on these results, we infer that the alkaline comets of UVC-exposed *Rev1*<sup>-/-</sup>*Xpc*<sup>-/-</sup> MEFs at the cell cycle of exposure represent ssDNA breaks, rather than DSBs resulting from collapsed replication forks.

To investigate whether the alkaline comets in UVC-exposed *Rev1<sup>-/-</sup>Xpc<sup>-/-</sup>* MEFs reflect ssDNA gaps opposite (6-4)PP, we adapted a recently described and highly sensitive immunostaining technique (Temviriyankul *et al.*, 2012b). As shown in Figure 4C, at 8 hours after exposure, mock-treated *Rev1<sup>-/-</sup>Xpc<sup>-/-</sup>* cells showed only background staining, similar to mock-treated or UVC-exposed *Xpc<sup>-/-</sup>* MEFs (Figs. 4A and B). However, after exposure to a dose as low as 0.4J/m<sup>2</sup> UVC (Fig. 4C), staining for unreplicated (6-4)PPs was observed in *Rev1<sup>-/-</sup>Xpc<sup>-/-</sup>* MEFs that were positive for EdU (i.e. replicating during UVC exposure) and negative for the mitotic marker H3<sup>ser10-P</sup>, in agreement with the notion that Rev1 is required for TLS of (6-4)PPs-containing ssDNA gaps (Jansen *et al.*, 2009). In non-mitotic, EdU-positive *Xpc<sup>-/-</sup>* cells (6-4)PPs embedded in ssDNA were not detected. This indicates that, at these UVC doses, most (6-4)PPs were efficiently bypassed in Rev1-proficient cells. Surprisingly, also EdU positive and mitotic, H3<sup>ser10-P</sup> positive, *Rev1<sup>-/-</sup>Xpc<sup>-/-</sup>* cells from this experiment displayed pronounced staining for (6-4)PPs, despite the highly condensed chromatin of mitotic chromosomes (Figs. 4D and E). Thus, we here provide direct proof that chromatin with (6-4)PP-containing ssDNA gaps, which were generated during S phase, can persist into mitosis.

To assess whether (6-4)PP within ssDNA are transferred through mitosis into the G1 phase of daughter nuclei, we immunostained for (6-4)PP in ssDNA in binucleated cells obtained as described above and in Fig. 4F. This revealed a more than 4-fold increase in (6-4)PPs in ssDNA in low-dose-exposed binucleated BrdU<sup>+</sup>/EdU<sup>-</sup> *Rev1<sup>-/-</sup>Xpc<sup>-/-</sup>* MEFs, as compared with mock treated MEFs (Fig. 4G). This result strongly suggests that patches of ssDNA containing (6-4)PPs can persist beyond mitosis, to the next cell cycle. Moreover, these ssDNA gaps are likely transferred from G1 into the 2<sup>nd</sup> S phase, since increased levels of (6-4)PPs in ssDNA were even found in low-dose-exposed binucleated BrdU<sup>+</sup>/EdU<sup>+</sup> *Rev1<sup>-/-</sup>Xpc<sup>-/-</sup>* MEFs (Fig. 4G). Alternatively, this result might suggest the generation of additional ssDNA gaps in *Rev1<sup>-/-</sup>Xpc<sup>-/-</sup>* MEFs following replication fork stalling at persistent (6-4)PPs in the 2<sup>nd</sup> S phase after UVC treatment.

### Unreplicated (6-4)PPs-Containing Cells Evade Checkpoint Signaling

It is commonly believed that cell cycle checkpoints prevent genomic instability (Cimprich *et al.*, 2008). We wondered whether DNA damage signaling was perturbed in *Rev1<sup>-/-</sup>Xpc<sup>-/-</sup>* MEFs, since these cells progressed to the subsequent cycle, resulting in S-phase-associated accumulation of DSBs and genomic instability, following low-dose UVC exposure. To investigate this, *Rev1<sup>-/-</sup>Xpc<sup>-/-</sup>* MEFs were pulse-labeled with EdU immediately before exposure to 0 or 0.4J/m<sup>2</sup> UVC, in order to mark cells that were replicating at the time of exposure. After exposure, the cells were cultured in the presence of nocodazole for 8h. Staining of cells for EdU and histone H3<sup>ser10-P</sup> revealed a population of *Rev1<sup>-/-</sup>Xpc<sup>-/-</sup>* MEFs that were EdU positive and H3<sup>ser10-P</sup> negative. These cells presumably represent pre-mitotic cells that were replicating during UVC exposure. These cells were tested for DNA damage signaling by quantifying the presence of Chk1<sup>S345-P</sup>, a downstream effector protein of activated Atr checkpoint kinase (Nam *et al.*, 2011) and also for chromatin-bound Rpa, an ssDNA-binding

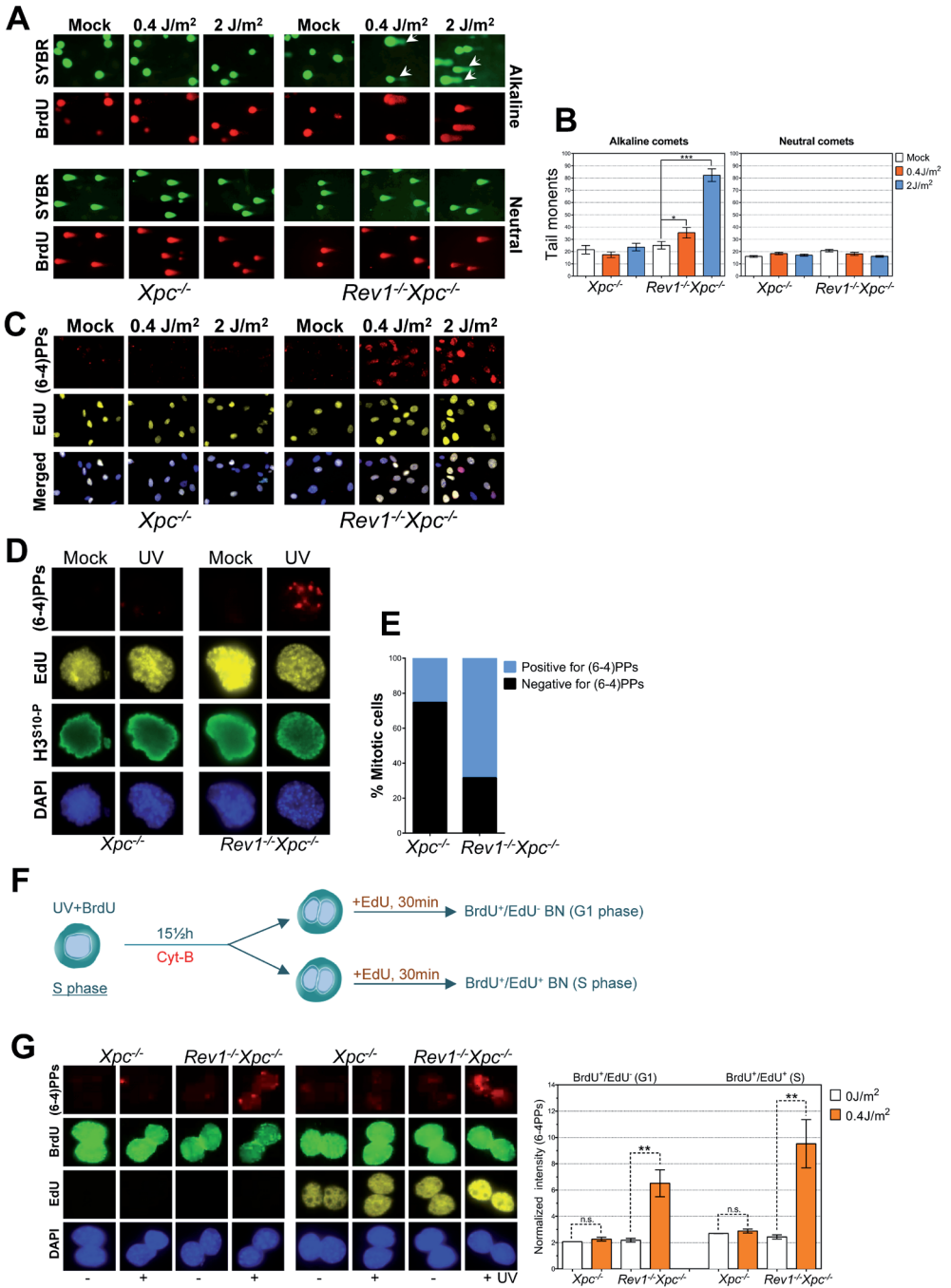


**Figure 4 | Patches of ssDNA containing unreplcated (6-4)PPs can persist beyond mitosis.** (A) ‘Comets’ of cells exposed to 0 - 2J/m<sup>2</sup> UVC, pulse-labeled with BrdU and arrested with nocodazole for 16h, before electrophoresis under alkaline (upper panels) or neutral (lower panels) condition. Nuclei were identified by

heterotrimeric protein that mediates Atr recruitment (Nam *et al.*, 2011). Enhanced levels of both proteins were only observed in low-dose UVC-exposed *Rev1<sup>-/-</sup>Xpc<sup>-/-</sup>* MEFs (Figs. 5A and B), suggesting that persisting ssDNA gaps containing (6-4)PP DNA induce significant damage signaling in the *Rev1<sup>-/-</sup>Xpc<sup>-/-</sup>* MEFs. However, this DNA damage signaling apparently does not prevent the cells to progress to the next cell cycle (Fig. 2). Significant levels of Chk1<sup>S345-P</sup> and chromatin-bound Rpa were also detected in the subsequent G1 phase of *Rev1<sup>-/-</sup>Xpc<sup>-/-</sup>* MEFs, whereas these levels further increased in the ensuing S phase (Figs. 5C and D; see Fig. 4F for a scheme).

To test whether the late appearance of MNs are caused by the formation of DSBs during the 2<sup>nd</sup> cell cycle following UVC exposure, we immunostained BrdU<sup>+</sup>/EdU<sup>-</sup> and BrdU<sup>+</sup>/EdU<sup>+</sup> binucleated *Rev1<sup>-/-</sup>Xpc<sup>-/-</sup>* MEFs for ATM<sup>S1980-P</sup>, which is associated with the early response to DSBs (Abraham *et al.*, 2005; Lee *et al.*, 2005). The intensity of the ATM<sup>S1981-P</sup> signal in BrdU<sup>+</sup>/EdU<sup>-</sup> binucleated *Rev1<sup>-/-</sup>Xpc<sup>-/-</sup>* MEFs was slightly increased after UV treatment (Fig. 5E), suggesting a low amount of UVC-induced DSB formation in G1 phase cells. Thus, although (6-4)PP in ssDNA gaps progress to the 2<sup>nd</sup> cell cycle after UVC exposure, they hardly collapse to DSBs before or during G1. However, significant staining for ATM<sup>S1980-P</sup> was detected in BrdU<sup>+</sup>/EdU<sup>+</sup> binucleated *Rev1<sup>-/-</sup>Xpc<sup>-/-</sup>* MEFs (Fig. 5E). Therefore, we conclude that DSBs are generated mainly during the 2<sup>nd</sup> S phase upon low-dose UVC-exposure, explaining the delayed genome instability upon low-dose UVC exposure. Since the intensity of ATM<sup>S1980-P</sup> signal in the 2<sup>nd</sup> S phase coincides with that of Chk1<sup>S345-P</sup> and chromatin-bound Rpa, we assume that at this stage DNA signaling results from ssDNA induced by enzymatic resection at DSBs (Symington *et al.*, 2011).

In conclusion, we provide evidence that, at low levels of UVC-induced DNA lesions, unreplicated DNA lesions are transmitted through mitosis into the subsequent cell cycle. During the ensuing S phase, these lesions are then converted into DSBs accompanied with massive DNA damage signaling. Finally, these DSBs underlie the formation of MN after the subsequent mitosis (Fig. 6 for a model).

- ▶ staining with SYBR and replicating cells at a time of UVC treatment were identified by immunostaining for BrdU. White arrows indicate the DNA discontinuities. **(B)** Tail moments in BrdU-positive cells for alkaline (left panel) or neutral 'comets' (right panel) ( $n=3$ ). Of note, tail moments of alkaline and neutral 'comets' are different due to the different settings that had to be applied for quantification purposes. **(C)** Immunostaining of cells under non-denaturing condition for (6-4)PPs, 8h after pulse-labeling with EdU for 30 min and exposure to 0 - 2J/m<sup>2</sup> UVC. Cells were co-immunostained for H3<sup>S10-P</sup> to exclude mitotic cells and EdU staining was performed to identify replicating cells. Only non-mitotic, H3<sup>S10-P</sup> negative, cells are shown. **(D)** Immunostaining under non-denaturing condition for the presence of (6-4)PPs and in nuclei of cells that were pulse-labeled with EdU, exposed to 0 - 2J/m<sup>2</sup> UVC and cultured in the presence of nocodazole for 16h. Cells were co-immunostained for H3<sup>S10-P</sup> to identify mitotic chromatin. **(E)** Quantification of (6-4)PPs-positive in mitotic cells (H3<sup>S10-P</sup>-positive cells) ( $n=3$ ). **(F)** Experimental scheme to discriminate binucleated (BN) cells that are in the second G1 phase (BrdU<sup>+</sup>/EdU<sup>-</sup> BN) from those that are in the second S phase (BrdU<sup>+</sup>/EdU<sup>+</sup> BN) after treatment with 0 or 0.4J/m<sup>2</sup> UVC. **(G)** Immunostaining under non-denaturing condition for (6-4)PPs in BrdU<sup>+</sup>/EdU<sup>-</sup> BN cells (G1 phase, left panel) and in BrdU<sup>+</sup>/EdU<sup>+</sup> BN cells (S phase, middle panel). Right panel depicts the quantification for fluorescence intensity. Error bar, SEM. Statistical significance was determined by Student's *t*-test. \*\*,  $p<0.01$ , n.s., non significant.

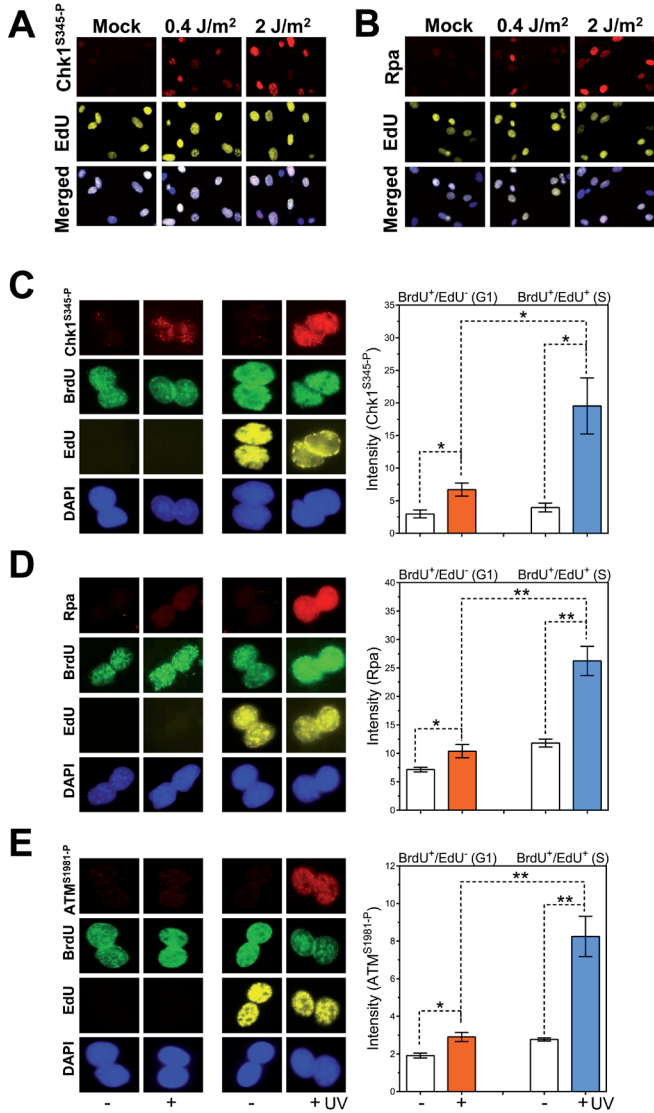


**Figure 5 | Checkpoint signaling in cells containing unrePLICATED (6-4)PPs.** (A-B) Immunostaining of *Rev1*<sup>-/-</sup>*Xpc*<sup>-/-</sup> cells, 8h after pulse-labeling with EdU for 30 min and exposure to 0 - 2J/m<sup>2</sup> UVC: (A) Chk1<sup>S345-P</sup>, and (B) Rpa. Cells were co-immunostained for H3<sup>S10-P</sup> to exclude mitotic cells and EdU staining was performed to identify replicating cells. Only non-mitotic cells are shown (C) Immunostaining for Chk1<sup>S345-P</sup> in BrdU<sup>+</sup>/EdU<sup>-</sup> *Rev1*<sup>-/-</sup>*Xpc*<sup>-/-</sup> BN cells (G1 phase, left panel) and in BrdU<sup>+</sup>/EdU<sup>+</sup> *Rev1*<sup>-/-</sup>*Xpc*<sup>-/-</sup> BN cells (S phase, middle panel). Right panel depicts the quantification for fluorescence intensity. (D) Immunostaining for Rpa in BrdU<sup>+</sup>/EdU<sup>-</sup> *Rev1*<sup>-/-</sup>*Xpc*<sup>-/-</sup> BN cells (G1 phase, left panel) and in BrdU<sup>+</sup>/EdU<sup>+</sup> *Rev1*<sup>-/-</sup>*Xpc*<sup>-/-</sup> BN cells (S phase, middle panel). Right panel depicts the quantification for fluorescence intensity. (E) Immunostaining for ATM<sup>S1981-P</sup> in BrdU<sup>+</sup>/EdU<sup>-</sup> *Rev1*<sup>-/-</sup>*Xpc*<sup>-/-</sup> BN cells (G1 phase, left panel) and in BrdU<sup>+</sup>/EdU<sup>+</sup> *Rev1*<sup>-/-</sup>*Xpc*<sup>-/-</sup> BN cells (S phase, middle panel). Right panel depicts the quantification for fluorescence intensity. Three independent experiments for each marker were performed and approximately 200 BN cells/ experiment were assayed. Error bar, SEM. Statistical significance was determined by Student's *t*-test. \*, *p*<0.05 \*\*, *p*<0.01

## DISCUSSION

In the present study we have analyzed the origins of genome instability in mammalian cells enduring replication stress following exposure to UV light, an important environmental carcinogen. We have found that patches of ssDNA containing (6-4)PPs in genomic DNA, following exposure to a low dose of UVC, can persist through G2 and mitosis. These ssDNA patches are transmitted to the subsequent cell cycle where they are converted into DSBs only during S phase.

These results contrast previous observations in human cells deficient for TLS polymerase Pol $\eta$  that display the rapid generation of DSBs after the formation of post-replicative ssDNA gaps following exposure to high-dose UVC light (Elvers *et al.*, 2011), possibly by Mus81/Eme1-dependent cleavage at stalled replication forks (Hanada *et al.*, 2007; Saintigny *et al.*, 2001). We hypothesize that at a high UV dose the massive generation of ssDNA may lead to depletion of Atr, which, in addition to DNA damage signaling, is involved in the stabilization of stalled replication forks (Elvers *et al.*, 2012). This will result in rapid fork collapse and the rapid, rather than delayed, formation of DSBs (Petermann *et al.*, 2010).

How are persistent ssDNA gaps converted into DSBs in the second cell cycle after UVC exposure? Immunostaining for Rpa and phosphorylated Chk1 in non-replicating BN cells (Figs. 5C and D) suggests that ssDNA gaps do activate the Rpa/Atr/Chk1 DNA damage signaling pathway (Fig. 5A and B). However, this does not result in the cessation of cell cycle progression. Moreover, the patches of ssDNA containing (6-4)PPs are not rapidly processed into DSBs, since the level of phosphorylated ATM is not enhanced in these cells, and MN are not observed following the cell cycle of UVC exposure. We therefore propose that, since ssDNA gaps persist through mitosis (Fig. 4D), during the subsequent S phase the replisome encounters gaps in the template, resulting in the generation of a DSB and consequently strong activation of the Rpa/Atr/Chk1 DNA damage signaling pathway (Figs. 5C, D and E). The concomitant phosphorylation of ATM suggests that DSBs arise during the second S phase, at these persisting ssDNA gaps.

So far, the transmission of structures, arising from replicative stress, through mitosis has been shown only after treatment of cells with DNA polymerase inhibitors and only in an indirect manner, *i.e.* by visualizing DNA damage response proteins such as  $\gamma$ -H2AX and 53BP1 (Ichijima *et al.*, 2010; Liu *et al.*, 2012; Lukas *et al.*, 2011). In contrast, our work provides a molecular description of the relevant DNA lesions (*i.e.* ssDNA gaps encompassing a photolesion), as well as a mechanistic basis for the resulting genomic instability, caused by environmentally relevant densities of DNA lesions. To the best of our knowledge, we provide for the first time physical evidence that patches of unreplicated DNA, at mutagenic and clastogenic DNA lesions, can be transferred through mitosis and transmitted to daughter cells, where they exert their clastogenic effects (Fig. 4D and G). We employed *Rev1<sup>-/-</sup>Xpc<sup>-/-</sup>* MEFs as a sensitive model, but it

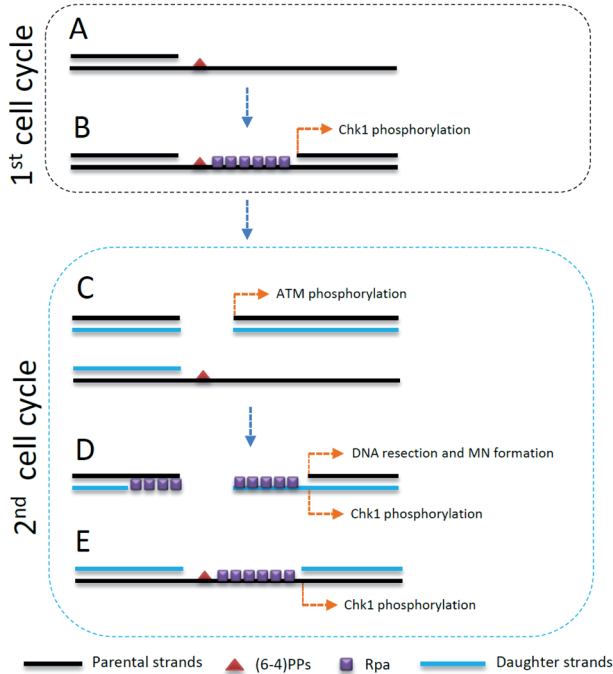


**Figure 6 | A schematic diagram representing the formation of DSBs from ssDNA patches in the second cell cycle. (A)** (6-4)PPs block DNA replication, resulting in the formation of ssDNA gaps. **(B)** Rpa binds to ssDNA gaps and subsequently Chk1 is activated *via* Atr signaling. Finally, ssDNA gaps are transmitted through mitosis to the next cell cycle. **(C)** Replication across ssDNA gaps leads to the formation of both DSBs and ssDNA containing (6-4)PPs. DSBs are eventually recognized by ATM to provoke DSB repair. **(D)** DSBs are resected, resulting in ssDNA, which is coated by Rpa. Persistent DSBs cause the formation of MN at the end of mitosis. **(E)** ssDNA coated with Rpa activates Atr signaling resulting in Chk1 phosphorylation.

should be emphasized that, at an equitoxic UVC dose, also *Xpc*<sup>-/-</sup> MEFs displayed delayed genome instability. This result suggests that the delayed mechanism of genome instability described here may represent a physiologically relevant mechanism.

In our study we used a low, physiologically relevant, dose of UVC as a model agent for the study of responses to both mild and severely helix-distorting DNA adducts. Such adducts are induced by many environmental genotoxic agents and cancer medicines, amongst others (Schut *et al.*, 1999; Sinha *et al.*, 2002). Our finding that genotoxic DNA damage can result in the induction of genomic instability only during the second S phase following exposure is highly relevant for clastogenicity testing of such compounds and provides a rationale for the recent chemical testing guidelines released by the Organisation for Economic Co-operation and Development (OECD), including (i) the standard *in vivo* MN test guideline 474 and (ii) the *in vitro* MN test guideline 487, which suggest that the first and the second cell divisions should be analyzed during MN analysis.

## MATERIALS AND METHODS

**Cell culture.** The generation of MEF lines deficient for Xpc (*Xpc*<sup>-/-</sup> MEFs) or double deficient for Xpc and Rev1 (*Rev1*<sup>-/-</sup>*Xpc*<sup>-/-</sup> MEFs) are described previously (Cheo *et al.*, 1997; Jansen *et al.*, 2009). Cells were grown in Dulbecco's modified Eagle's medium (DMEM) containing 4.5 g/l glucose, Glutamax and pyruvate (Invitrogen), supplemented with 10% fetal calf serum, penicillin (100 U/ml), and streptomycin (100 µg/ml) (DMEM medium) at 37 °C in a humidified atmosphere containing 5% CO<sub>2</sub>.

**Clonogenic survival assay.** MEFs were treated with UVC doses up to 5J/m<sup>2</sup>, trypsinized, and counted. A fixed number of cells was plated in p90 dishes and cultured for 10 days at 5% CO<sub>2</sub> and 37°C. Before staining with methylene blue, cells were washed and fixed. To determine the relative clonogenic survival, the cloning efficiency of unexposed cells was set at 100%.

**Cytokinesis-blocked micronucleus assay.** The assay was performed as previously described (Temviriyankul *et al.*, 2012a; Temviriyankul *et al.*, 2012b), which method was based on previous studies (Bolt *et al.*, 2011; Fenech, 1993). Briefly,  $7.5 \times 10^4$  cells were plated on a glass slide (76 mm × 26 mm) and cultured overnight. Prior to exposure to 0 - 5J/m<sup>2</sup> UVC, cells were washed twice with PBS. At 0h or 24h after UVC treatment, Cytochalasin B (cyt-B) (3 µg/ml) (Sigma-Aldrich) was added to the cultures in order to inhibit cytokinesis. Twenty-four hours after addition of cyt-B, cells were fixed using 3.5% paraformaldehyde (4°C) and 0.5% Triton-X100. Then, slides were rinsed with PBS and nuclei were stained with DAPI (17.5 ng/ml). The slides were soaked in 70%, 90% and absolute ethanol for 5 min each, respectively. The binucleated cells (BN) and number of micronuclei (MN) were scored using a fluorescence microscope (Zeiss, Germany) and the Metafer 4 program (Metasystem, Germany). Three independent experiments were performed and mock treated cells were included as a control. To determine whether MN result from DNA breaks in the first or second cell cycle after UVC exposure, the formation of MN was determined in two groups of cells. In the first group, immediately after 0 - 0.4J/m<sup>2</sup> UVC irradiation, cells were treated with 10 µM Bromodeoxyuridine (BrdU, Millipore) for 30 min after which the cells were cultured in the presence of cyt-B for 23h to generate BN cells. Thus, MN in BN cells with nuclei containing BrdU are derived from S phase cells at the time of UV exposure (first cell cycle MN). To distinguish BN cells with nuclei in G1 phase from those that have entered a new S phase, the cells were incubated in medium containing 10 µM 5-ethynyl-2'-deoxyuridine (EdU, Invitrogen) for 30 min, prior to fixation. Consequently, BN cells with nuclei double positive for BrdU and EdU reflect 2<sup>nd</sup> S phase cells after UVC exposure. In the second group, immediately after UVC irradiation, cells were pulse labeled with 10 µM Bromodeoxyuridine (BrdU, Millipore) for 30 min, after which the cells were cultured in DMEM medium for 23h without cyt-B, to allow cells to enter the second S phase after UVC exposure. Then, EdU was added and 30 min later, cells were washed with PBS and cultured in the presence of cyt-B for 24h to generate BN cells. MN in BN cells with nuclei containing both BrdU and EdU are derived in cells that have completed two rounds of DNA replication (second cell cycle MN). To visualize BrdU and EdU in DNA of BN cells, the DNA of nuclei was denatured, incorporation of EdU was determined according to the manufacturer's protocol, whereas incorporation of BrdU was detected by immunofluorescence. Then, BN cells were scored for MN.

**Bivariate cell cycle analysis.** MEFs were seeded in 90 mm dishes at 70% confluence and were cultured overnight. Cells were rinsed with PBS and exposed to UVC or mock treated. Immediately after exposure to 0 - 2J/m<sup>2</sup> UVC, cells were pulse labeled with BrdU for 30 min in 5% CO<sub>2</sub> at 37°C. Cells were trypsinized and fixed with 70% ethanol at indicated time points. BrdU staining and flow cytometry were performed as described (Temviriyankul *et al.*, 2012b).

**Single cell gel electrophoresis assay (Comet assay).** DNA strand interruptions and DSBs in replicating cells at a time of UVC exposure were measured by alkaline and neutral comet assay, respectively. In detail, cells were plated to reach about 60-70% confluence. To identify replicating cells at the time of UVC treatment, cells were pulse-labeled for 30 min with BrdU, immediately after exposure to 0 - 2J/m<sup>2</sup> UVC. Then, the cell population was cultured in the presence of the mitotic spindle poison Nocodazole (300ng/ml) for 16h to accumulate cells in G2/M phase. Single cell suspensions were processed to visualize comets according to the manufacturer's instructions (Trevigen). In order to visualize BrdU-containing chromatin after gel electrophoresis, chromatin was denatured and stained for BrdU using a mouse monoclonal antibody against BrdU (Becton Dickinson) followed by incubation with an Alexafluor555-labeled goat-anti-mouse antibody (Invitrogen). Staining with SYBR green (Invitrogen) was applied to visualize DNA. The comet tail moments of about 180-240 BrdU-containing nuclei from three independent experiments were scored using the Comet software (TriTek).

**Immunofluorescence.** The antibodies used in immunofluorescence were mouse anti-BrdU (Beckton Dickinson), rabbit anti-BrdU (Rockland immunochemicals), mouse anti-Histone H3<sup>S10-P</sup> (Millipore), rabbit anti-Histone H3<sup>S10-P</sup> (Millipore), mouse anti-(6-4)PP (CosmoBio), rabbit anti-Chk1<sup>S345-P</sup> (Cell signaling), rat anti-Rpa (Cell signaling), mouse anti-ATM<sup>S1981-P</sup> (Rockland immunochemicals), and appropriate secondary antibodies conjugated with fluorescence dyes (Invitrogen). To detect (6-4)PPs, Rpa and Chk1<sup>S345-P</sup> in the late S/G2 phase, cells were seeded on coverslips and cultured overnight in 5% CO<sub>2</sub> at 37°C. Prior to exposure to 0 - 2J/m<sup>2</sup> UVC, cells were pulse-labeled with EdU for 30 min. After UV exposure, cells were cultured in the presence of nocodazole for 8h, to prevent cells from entering a second cell cycle after UV exposure. Then cells were fixed and immunostained for (6-4)PPs, Rpa or Chk1<sup>S345-P</sup> using appropriate antibodies. To increase the sensitivity of anti-(6-4)PPs staining, Tyramine Signal Amplification (TSA, Perkin-Elmer) was applied, according to the manufacturer's recommendations. The late S/G2 phase cells that were replicating at the time of UV exposure were identified by positive staining for EdU and negative staining for H3<sup>S10-P</sup>. To detect (6-4)PPs in mitotic cells, cell cultures were treated as described above, with the exception that the cells were cultured in nocodazole-containing medium for 16h to accumulate G2/M phase cells. The mitotic cells, which were replicating at a time of UVC treatment, were identified by positive staining for both EdU and H3<sup>S10-P</sup>. (6-4)PPs and DNA damage response proteins in BN cells were visualized as follows. Cells were cultured on coverslips in medium with 10 μM BrdU for 30 min, immediately after irradiation with 0-0.4J/m<sup>2</sup> UVC. Then, cells were cultured in the presence of cyt-B for 15½h. Prior to fixation, cells were pulse-labeled with 10 μM EdU in the presence of cyt-B for 30 min. Since BrdU detection requires a denaturation step, which may destroy protein epitopes, fixed cells were firstly stained for EdU. Then, cells were blocked with 5% BSA+0.1% tween-20 in PBS for 30 min and subsequently incubated overnight with anti-Rpa, Chk1<sup>S345-P</sup> or ATM<sup>S1981-P</sup> antibodies diluted in 1% BSA+0.1% tween-20 in PBS at 4°C. Then, appropriate secondary antibodies were applied. After washing, cells were again fixed with 3.7% Paraformaldehyde for 15 min, followed by incubation with 2N HCl for 12 min, in order to denature DNA. Before incubation with anti-BrdU antibodies, coverslips were rinsed intensively to reduced acidity. After incubation with an appropriate secondary antibody against anti-BrdU antibodies, nuclei were stained with DAPI. Images were captured using a wide-field microscope (Axioplan 2, or Axioplan Imager M2, Zeiss). Image intensity was quantified using Fiji (ImageJ) software (National Institutes of Health).

## ACKNOWLEDGEMENTS

This work was supported by a PhD scholarship to P.T. under the project Strategic Frontier Research (SFR-4) from the Office of the Higher Education Commission, the Royal Thai Government, Thailand.

SUPPLEMENTARY FIGURE

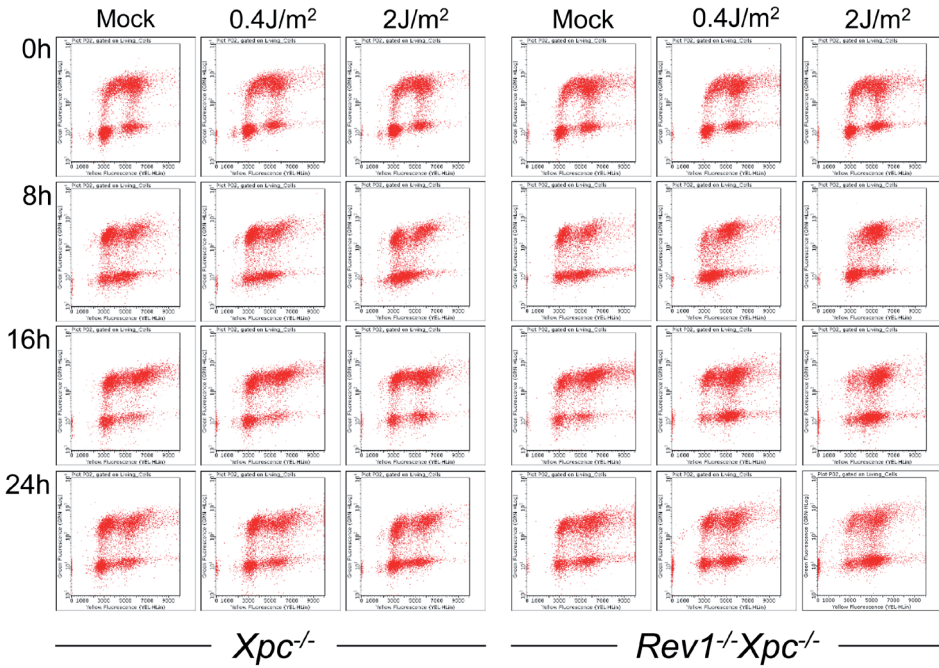


**Figure S1 | *Rev1*<sup>-/-</sup>*Xpc*<sup>-/-</sup> MEFs can progress to the second cell cycle upon low doses of UVC irradiation.** Cells were pulse-labeled with BrdU, immediately after UVC exposure (up to 2J/m<sup>2</sup>) or mock-treated. At indicated times after exposure, cells were fixed. Then, BrdU incorporation was determined by immunostaining and DNA content was measured using propidium iodide (PI). FACS profiles were generated by flow cytometer and BrdU-positive cells in G1, S and late S/G2 phases were quantified.

## REFERENCES

- Abraham RT**, Tibbetts RS (2005). Guiding ATM to broken DNA. *Science*. **308**: 510-511
- Berdichevsky A**, Izhar L, Livneh Z (2002). Error-free recombinational repair predominates over mutagenic translesion replication in *E. coli*. *Mol Cell*. **10**: 917-924
- Bolt HM**, Stewart JD, Hengstler JG (2011). A comprehensive review about micronuclei: mechanisms of formation and practical aspects in genotoxicity testing. *Arch Toxicol*. **85**: 861-862
- Bonassi S**, Znaor A, Ceppi M, Lando C, Chang WP, Holland N, Kirsch-Volders M, Zeiger E, Ban S, Barale R *et al.* (2007). An increased micronucleus frequency in peripheral blood lymphocytes predicts the risk of cancer in humans. *Carcinogenesis*. **28**: 625-631
- Chapman JR**, Taylor MR, Boulton SJ (2012). Playing the end game: DNA double-strand break repair pathway choice. *Mol Cell*. **47**: 497-510
- Cheo DL**, Ruven HJ, Meira LB, Hammer RE, Burns DK, Tappe NJ, van Zeeland AA, Mullenders LH, Friedberg EC (1997). Characterization of defective nucleotide excision repair in XPC mutant mice. *Mutat Res*. **374**: 1-9
- Cimprich KA**, Cortez D (2008). ATR: an essential regulator of genome integrity. *Nat Rev Mol Cell Biol*. **9**: 616-627
- Daigaku Y**, Davies AA, Ulrich HD (2010). Ubiquitin-dependent DNA damage bypass **is separable** from genome replication. *Nature*. **465**: 951-955
- Diamant N**, Hendel A, Vered I, Carell T, Reissner T, de Wind N, Geacintov N, Livneh Z (2012). DNA damage bypass operates in the S and G2 phases of the cell cycle and exhibits differential mutagenicity. *Nucleic Acids Res*. **40**: 170-180
- Elvers I**, Hagenkorf A, Johansson F, Djureinovic T, Lagerqvist A, Schultz N, Stoimenov I, Erixon K, Helleday T (2012). CHK1 activity is required for continuous replication fork elongation but not stabilization of post-replicative gaps after UV irradiation. *Nucleic Acids Res*. **40**: 8440-8448
- Elvers I**, Johansson F, Groth P, Erixon K, Helleday T (2011). UV stalled replication forks restart by re-priming in human fibroblasts. *Nucleic Acids Res*. **39**: 7049-7057
- Estensen RD** (1971). Cytochalasin B. I. Effect on cytokinesis of Novikoff hepatoma cells. *Proc Soc Exp Biol Med*. **136**: 1256-1260
- Fenech M** (1993). The cytokinesis-block micronucleus technique: a detailed description of the method and its application to genotoxicity studies in human populations. *Mutat Res*. **285**: 35-44
- Fournier RE**, Pardee AB (1975). Cell cycle studies of mononucleate and cytochalasin-B--induced binucleate fibroblasts. *Proc Natl Acad Sci U S A*. **72**: 869-873
- Hanada K**, Budzowska M, Davies SL, van Druenen E, Onizawa H, Beverloo HB, Maas A, Essers J, Hickson ID, Kanaar R (2007). The structure-specific endonuclease Mus81 contributes to replication restart by generating double-strand DNA breaks. *Nat Struct Mol Biol*. **14**: 1096-1104
- Ichijima Y**, Yoshioka K, Yoshioka Y, Shinohe K, Fujimori H, Unno J, Takagi M, Goto H, Inagaki M, Mizutani S *et al.* (2010). DNA lesions induced by replication stress trigger mitotic aberration and tetraploidy development. *PLoS One*. **5**: e8821
- Izhar L**, Goldsmith M, Dahan R, Geacintov N, Lloyd RG, Livneh Z (2008). Analysis of strand transfer and template switching mechanisms of DNA gap repair by homologous recombination in *Escherichia coli*: predominance of strand transfer. *J Mol Biol*. **381**: 803-809
- Izhar L**, Ziv O, Cohen IS, Geacintov NE, Livneh Z (2013). Genomic assay reveals tolerance of DNA damage by both translesion DNA synthesis and homology-dependent repair in mammalian cells. *Proc Natl Acad Sci U S A*. **110**: E1462-1469
- Jansen JG**, Tsaalbi-Shtylik A, Hendriks G, Gali H, Hendel A, Johansson F, Erixon K, Livneh Z, Mullenders LH, Haracska L *et al.* (2009). Separate domains of Rev1 mediate two modes of DNA damage bypass in mammalian cells. *Mol Cell Biol*. **29**: 3113-3123
- Lee JH**, Paull TT (2005). ATM activation by DNA double-strand breaks through the Mre11-Rad50-Nbs1 complex. *Science*. **308**: 551-554
- Liu S**, Opiyo SO, Manthey K, Glanzer JG, Ashley AK, Amerin C, Troksa K, Shrivastav M, Nickoloff JA, Oakley GG (2012). Distinct roles for DNA-PK, ATM and ATR in RPA phosphorylation and checkpoint activation in response to replication stress. *Nucleic Acids Res*. **40**: 10780-10794
- Lukas C**, Savic V, Bekker-Jensen S, Doil C, Neumann B, Pedersen RS, Grofte M, Chan KL, Hickson ID, Bartek J *et al.* (2011). 53BP1 nuclear bodies form around DNA lesions generated by mitotic transmission of chromosomes under replication stress. *Nat Cell Biol*. **13**: 243-253
- McKelvey-Martin VJ**, Green MH, Schmezer P, Pool-Zobel BL, De Meo MP, Collins A (1993). The single cell gel electrophoresis assay (comet assay): a European review. *Mutat Res*. **288**: 47-63

- Murgia E**, Ballardini M, Bonassi S, Rossi AM, Barale R (2008). Validation of micronuclei frequency in peripheral blood lymphocytes as early cancer risk biomarker in a nested case-control study. *Mutat Res.* **639**: 27-34
- Nam EA**, Cortez D (2011). ATR signalling: more than meeting at the fork. *Biochem J.* **436**: 527-536
- Osman F**, Whitby MC (2007). Exploring the roles of Mus81-Eme1/Mms4 at perturbed replication forks. *DNA Repair (Amst).* **6**: 1004-1017
- Petermann E**, Helleday T (2010). Pathways of mammalian replication fork restart. *Nat Rev Mol Cell Biol.* **11**: 683-687
- Saintigny Y**, Delacote F, Vares G, Petitot F, Lambert S, Averbeck D, Lopez BS (2001). Characterization of homologous recombination induced by replication inhibition in mammalian cells. *EMBO J.* **20**: 3861-3870
- Sale JE**, Lehmann AR, Woodgate R (2012). Y-family DNA polymerases and their role in tolerance of cellular DNA damage. *Nat Rev Mol Cell Biol.* **13**: 141-152
- Schut HA**, Snyderwine EG (1999). DNA adducts of heterocyclic amine food mutagens: implications for mutagenesis and carcinogenesis. *Carcinogenesis.* **20**: 353-368
- Sinha RP**, Hader DP (2002). UV-induced DNA damage and repair: a review. *Photochem Photobiol Sci.* **1**: 225-236
- Symington LS**, Gautier J (2011). Double-strand break end resection and repair pathway choice. *Annu Rev Genet.* **45**: 247-271
- Szuts D**, Marcus AP, Himoto M, Iwai S, Sale JE (2008). REV1 restrains DNA polymerase zeta to ensure frame fidelity during translesion synthesis of UV photoproducts in vivo. *Nucleic Acids Res.* **36**: 6767-6780
- Temviriyankul P**, Meijers M, van Hees-Stuivenberg S, Boei JJ, Delbos F, Ohmori H, de Wind N, Jansen JG (2012a). Different sets of translesion synthesis DNA polymerases protect from genome instability induced by distinct food-derived genotoxins. *Toxicol Sci.* **127**: 130-138
- Temviriyankul P**, van Hees-Stuivenberg S, Delbos F, Jacobs H, de Wind N, Jansen JG (2012b). Temporally distinct translesion synthesis pathways for ultraviolet light-induced photoproducts in the mammalian genome. *DNA Repair (Amst).* **11**: 550-558
- Washington MT**, Minko IG, Johnson RE, Haracska L, Harris TM, Lloyd RS, Prakash S, Prakash L (2004). Efficient and error-free replication past a minor-groove N2-guanine adduct by the sequential action of yeast Rev1 and DNA polymerase zeta. *Mol Cell Biol.* **24**: 6900-6906
- Waters LS**, Minesinger BK, Wiltout ME, D'Souza S, Woodruff RV, Walker GC (2009). Eukaryotic translesion polymerases and their roles and regulation in DNA damage tolerance. *Microbiol Mol Biol Rev.* **73**: 134-154
- Waters LS**, Walker GC (2006). The critical mutagenic translesion DNA polymerase Rev1 is highly expressed during G(2)/M phase rather than S phase. *Proc Natl Acad Sci U S A.* **103**: 8971-8976
- Yang IY**, Hashimoto K, de Wind N, Blair IA, Moriya M (2009). Two distinct translesion synthesis pathways across a lipid peroxidation-derived DNA adduct in mammalian cells. *J Biol Chem.* **284**: 191-198
- Zhang Y**, Wu X, Rechkoblit O, Geacintov NE, Taylor JS, Wang Z (2002). Response of human REV1 to different DNA damage: preferential dCMP insertion opposite the lesion. *Nucleic Acids Res.* **30**: 1630-1638
- Zhao B**, Wang J, Geacintov NE, Wang Z (2006). Poleta, Polzeta and Rev1 together are required for G to T transversion mutations induced by the (+)- and (-)-trans-anti-BPDE-N2-dG DNA adducts in yeast cells. *Nucleic Acids Res.* **34**: 417-425

